International Journal of Pharmaceutics 385 (2010) 187–193

Contents lists available at ScienceDirect

International Journal of Pharmaceutics

journal homepage: www.elsevier.com/locate/ijpharm

Pharmaceutical Nanotechnology

Transcutaneous delivery of a nanoencapsulated antigen: Induction of immune responses

George Mattheolabakis[a], George Lagoumintzis[b], Zoi Panagi[a], Evangelia Papadimitriou[c], Charalambos D. Partidos[d], Konstantinos Avgoustakis[a,*]

[a] Laboratory of Pharmaceutical Technology, Department of Pharmacy, University of Patras, Rio 26500, Greece
[b] Laboratory of Molecular Biology and Immunology, Department of Pharmacy, University of Patras, Rio 26500, Greece
[c] Laboratory of Molecular Pharmacology, Department of Pharmacy, University of Patras, Rio 26500, Greece
[d] Inviragen, 6502 Odana Rd, Suite 200, Madison, WI 53719, USA

ARTICLE INFO

Article history:
Received 27 March 2009
Accepted 17 October 2009
Available online 27 October 2009

Keywords:
Skin
Antigen
PLA
Nanoparticles
Immunization
Ovalbumin
Transcutaneous

ABSTRACT

We investigated the influence of antigen entrapment in PLA nanoparticles on the immune responses obtained after transcutaneous immunization. OVA-loaded PLA nanoparticles were prepared using a double emulsion process. Following application onto bare skin of mice in vivo, fluorescence-labeled nanoparticles were detected in the duct of the hair follicles indicating that the nanoparticles can penetrate the skin barrier through the hair follicles. Although the OVA-loaded nanoparticles elicited lower antibody responses than those induced by OVA in aqueous solution they were more efficient in inducing cytokine responses. *In vitro* re-stimulation of cultured splenocytes with OVA elicited a little higher levels of IFN-γ (difference statistically insignificant, $p > 0.05$) and significantly higher levels of IL-2 ($p < 0.001$) in mice immunized with OVA-loaded nanoparticles compared to those immunized with OVA in solution. In the presence of CT, the OVA-loaded nanoparticles induced significantly higher IFN-γ and IL-2 than all other formulations. Transcutaneous administration of OVA encapsulated in the PLA nanoparticles exhibited priming efficacy to a challenging dose of OVA given via different route. These findings indicate the potential of nanoparticles to deliver antigens via the transcutaneous route and prime for antibody and strong cellular responses. The co-administration of an adjuvant such as CT had the added advantage of modulating the immune response, a desirable characteristic within the context of vaccination against intracellular versus extracellular pathogens.

1. Introduction

One of the major impediments to ensuring vaccine efficacy is that of delivery. Towards this goal, innovative vaccination strategies are currently under study and development, including transcutaneous immunization (Glenn et al., 1998; Beignon et al., 2001) or skin immunization using jet injectors (Guidice and Campbell, 2006). Skin is an attractive route for vaccination due to its accessibility, abundance of powerful antigen-presenting cells (APCs) (Streilein, 1983), and potential for non-invasive delivery. The development of methods that enable the simple and non-invasive administration of vaccines could help in overcoming certain barriers to mass vaccination campaigns, such as the requirement for trained medical personnel, the use of contaminated needles, and issues related to the cold-chain transport and storage of vaccines.

In recent years, Poly(lactide) (PLA) and Poly(lactide-co-glycolide) (PLGA) microparticles have been extensively studied as an antigen delivery system. Immunization with various types of antigens entrapped in PLGA microparticles elicited enhanced and long-lasting humoral and cellular immune responses (O'Hagan et al., 1993; Men et al., 1996; Igartua et al., 1998; Rosas et al., 2002; Nikou et al., 2005). Based on *in vitro* skin permeation studies, nanoparticles have been shown to penetrate the pig skin (Alvarez-Roman et al., 2004; Kohli and Alpar, 2004; Lademann et al., 2007). This capacity appears to be influenced by the size and charge of the particles. With regard to the particle size, Vogt et al. (2006) reported that transcutaneously applied 40 nm nanoparticles (fluorescent FluoSpheres), but not 750 or 1500 nm (Fluoresbrite Carboxylate particles), penetrated the human skin stripped by approx. 30% of its stratum corneum using cyanacrylate. The particles were shown to enter in epidermal Langerhans cells *in vitro*. Based on these findings, we opted to examine the potential of PLA nanoparticles as a vector for antigen delivery via the transcutaneous route. As a model antigen we used the ovalbumin (OVA) and characterized the humoral and cellular responses induced.

* Corresponding author. Tel.: +30 2610 969330; fax: +30 2610 996302.
E-mail address: avgoust@upatras.gr (K. Avgoustakis).

0378-5173/$ – see front matter © 2009 Elsevier B.V. All rights reserved.
doi:10.1016/j.ijpharm.2009.10.033

2. Materials and methods

2.1. Materials

D,L-Lactide was purchased from Polysciences (USA). OVA, albumin-fluorescein isothiocyanate conjugate (FITC-albumin) and CT were obtained from Sigma (USA). The goat anti-mouse immunoglobulin IgG labeled with horseradish peroxidase (HRP) was obtained from Serotec (United Kingdom). The ELISA kits for mouse IL-2, IL-4, IL-10 and IFN-γ were purchased from Diaclone (France). All chemicals and solvents used were at least of analytical grade.

2.2. Polymer synthesis

PLA ($M_W = 109 \times 10^3$, polydispersity index = 3.2) was synthesized by melt polymerization under nitrogen of D,L-lactide using stannous octoate as catalyst (Beletsi et al., 1999).

2.3. Preparation and characterization of nanoparticles

OVA-loaded PLA nanoparticles were prepared by a double emulsion process. Briefly, OVA (10 mg) was dissolved in water (400 μl), and the solution was emulsified in a polymer solution in dichloromethane (50 mg polymer in 2 ml solvent) using probe sonication (Bioblock Scientific, model 75038) at 15 W for 1 min. This emulsion was transferred to an aqueous solution of sodium cholate (6 ml, 12 mM) and the mixture was probe-sonicated at 15 W for 1 min. The w/o/w emulsion formed was gently stirred at room temperature in a fume hood for 6 h. The nanoparticles were purified by centrifugation and the pellet was reconstituted in fresh water and filtered through a 1.2 μm filter (Millex AP, Millipore) to remove aggregates possibly formed during nanoparticle preparation. The nanoparticles were freeze-dried after mixing with trehalose in a 2:1 trehalose:nanoparticles weight ratio and stored in a dessicator until used.

The size and the ζ (zeta) potential of the nanoparticles were determined using photon correlation spectroscopy (pcs) and microelectrophoresis, respectively, using a Malvern Nano ZS instrument. The ζ potential was measured with the nanoparticles suspended in 1 mM KCl. Atomic force microscopy (AFM) observation was performed in air at room temperature, on a Dimension 3000 apparatus, as well as on Multimode Equipment, both monitored by a Nanoscope IIIa controller from Digital Instruments (Santa Barbara, CA, USA). A droplet (5 μL) of sample from lyophilized and reconstituted in water nanoparticles was deposited on a freshly cleaved mica surface, spread and partially dried with a stream of argon. The images were obtained in tapping mode, using commercial silicon probes, from Nanosensors, with cantilevers having a length of 228 μm, resonance frequencies of 75–98 kHz, spring constants of 29–61 N/m and a nominal tip curvature radius of 5–10 nm. The scan rate used was 1 Hz.

The loading of the nanoparticles with OVA was determined after their hydrolysis using the bicinchoninic acid (BCA) assay. Briefly, lyophilized samples of purified nanoparticles were hydrolyzed in 0.1N NaOH (37 °C) for 24 h and the protein content in the resulting solutions was determined with the BCA method (Smith et al., 1985).

Fluorescent PLA nanoparticles labeled with FITC-albumin (Sigma) were prepared by an emulsification-solvent evaporation technique. FITC-albumin (4 mg) was dissolved in 400 μl water and emulsified in a 2 ml solution of PLA (50 mg) in dichloromethane (2 ml) using probe sonication at 15 W for 1 min. The emulsion was transferred to an aqueous solution of sodium cholate (6 ml, 12 mM) and the mixture was probe-sonicated at 15 W for 1 min. The w/o/w emulsion formed was gently stirred at room temperature in a fume hood for 6 h. The nanoparticles were purified by centrifugation and reconstitution of the pellet in fresh water and filtered through a 1.2 μm filter (Millex AP, Millipore).

2.4. Measurement of OVA retention in nanoparticles in vitro

Samples of OVA-loaded nanoparticles (2–3 mg total protein content) were transferred to 30 ml PBS (pH 7.4) and incubated in a mildly shaking water bath (37 °C). At predetermined time intervals, 500 μl samples were withdrawn and centrifuged (28,000 rpm, 30 min). The supernatants were assayed for protein by the BCA method. Fresh incubation medium (500 μl) was added to the nanoparticles after each sampling.

2.5. Study of nanoparticle penetration into the skin

Female BALB/c mice 6–8 weeks old (18–24 g) were anesthetized with a subcutaneous injection of 110 μg ketamine/g mouse and 11 μg xylazine/g mouse. Most of the hair from the back of each mouse was removed with a Panasonic ER 140H hair trimmer and then wetted with soap-water and shaved with a commercial shaving blade. Neither cuts nor skin irritation was observed. The shaved area was wiped with a cotton pad. Half an hour later, PLA nanoparticles labeled with FITC-albumin (100 μl, 0.6 mg solids content) were uniformly applied onto the shaved area (approx. 2.25 cm^2, 1.5 cm × 1.5 cm) using a pipette tip. Half an hour later, mice were sacrificed, their back was washed twice with water and dried with a cotton swab. Samples (1 cm^2) from the treated skin areas were removed and frozen in isopentane (−60 °C) for 5 min. Sections 20 μm thick were cut using a LEICA CM 1500 cryotome, and collected on a glass slide, covered with Mowiol 488 and photographed using a LEICA DM I6000B confocal laser microscope equipped with a LEICA TCS SP5 laser scanner. Laser excitation wavelengths of 568 and 488 nm were used separately to scan skin and fluorescent nanoparticles, respectively. The fluorescence emanating from the skin appeared red-colored (auto-fluorescence) and that originating from the fluorescent nanoparticles appeared green-colored; the images were overlaid to provide dual-colored images (Alvarez-Roman et al., 2004).

2.6. Immunization

Female BALB/c mice 6–8 weeks old (18–24 g) were used in all experiments. All animal experiments were conducted in accordance to the national regulations for care and use of laboratory animals.

Groups of seven mice were immunized by topical application of different OVA formulations (each containing 200 μg OVA). Prior to immunization mice were shaved as described in the previous paragraph and the antigen formulations were applied onto the shaved skin areas (approx. 2.25 cm^2) with the tip of a pipette. After 1 h, the shaved skin area was washed with water and dried with a cotton swab. Cholera toxin (CT) (50 μg/mouse) was included in certain formulations as adjuvant. An equal booster dose of each formulation was administered by the same route 2 weeks later. The following groups were included in the study: (A) OVA solution in water, (B) OVA solution in water plus CT, (C) OVA entrapped in PLA nanoparticles, (D) OVA entrapped in PLA nanoparticles plus CT, and (E) non-immunized mice. Blood samples were collected 2 and 4 weeks after the primary immunization. Just after the second blood sampling (4 weeks after priming), 3 mice from each group were sacrificed and their spleens were excised, whereas the remaining 4 mice per group were injected subcutaneously with 50 μl of a 1 mg/ml OVA solution in water. Two weeks later, the subcutaneously immunized mice were sacrificed and blood samples were obtained.

The protocol for raising the hyperimmune antiserum involved a primary immunization of mice with 200 μg OVA dissolved in 50 μl saline and mixed at 1:1 (v/v) with Freund's Complete Adjuvant (FCA) (Difco). Mice were injected subcutaneously (50 μl of the mixture in each flank of mice back), and received two booster immunizations of the same dose of antigen emulsified 1:1 (v/v) in Freund's Incomplete Adjuvant (FIA) (Difco), 2 and 4 weeks after the primary injection. Mice were bled by cardiac puncture 7 days after the final immunization.

2.7. Analysis of the immune response

The anti-OVA antibody responses were measured in serum samples of immunized mice by ELISA. Briefly, microtiter plates (Costar) were coated overnight with 5 μg/ml OVA in carbonate-bicarbonate buffer (0.05 M, pH 9.6, 100 μl/well) at room temperature. Non-specific binding sites were blocked with PBS containing 2% BSA (Sigma). Serum samples, at dilutions from 1:100 to 1:1000, and hyperimmune serum samples, at 1:1000 and 1:10,000 dilutions, were added to wells and incubated overnight. After washing, microtiter plates were incubated with 100 μl/well of HRP-conjugated goat anti-mouse IgG antiserum (Sigma). TMB (100 μl/well) was added, followed by incubation at room temperature for 15 min. The reaction was stopped by the addition of 100 μl of 1 M H_2SO4 solution in each well and the absorbance was measured at 450 nm. The results were expressed as antibody titers, i.e. as the antiserum dilution providing an absorbance of 0.2 (±SD).

OVA-specific proliferative responses were determined in splenocyte cultures using the [^{3}H]thymidine incorporation assay (Nikou et al., 2005). Spleens were aseptically removed and pooled for each group of animals. Then, they were minced using a pair of scissors and passed through a fine steel mesh to obtain a homogeneous cell suspension. Erythrocytes were lysed with ammonium chloride (0.8%, w/v). After centrifugation (500 × *g* at 4 °C for 10 min), the pelleted cells were washed three times in PBS, and re-suspended in RPMI 1640 medium (Gibco) supplemented with 10% (v/v) FCS (fetal calf serum), 4 mM L-glutamine, 50 μM 2-mercaptoethanol and 100 μg/ml gentamycine. Cells were plated at 5×10^5 cells/well (in pentaplicates) in U-bottomed 96-well plates (200 μl medium/well) and stimulated with OVA (50 μg/ml final concentration in the wells). Culture plates were incubated into a cell incubator (5% CO_2, 100% RH, 37 °C) for 48 h. At 18 h before the end of the incubation period, 1 μCi of [^{3}H]thymidine was added into each well. Cells were harvested, washed twice with ice-cooled PBS and then (twice) with ice-cooled trichloroacetic acid (5%, w/v in water). Finally, the cells were dissolved in 0.5 ml NaOH (0.2N) and the radioactivity of the obtained solutions after dilution in CytoScint (MP, USA) scintillation fluid was measured in a Wallac 1410 liquid scintillation counter. Non-stimulated cells were used as negative control and cells stimulated with 5 μg/ml. Concanavalin A were used as positive control. The results were expressed as stimulation indices (SI) of the mean counts per minute (cpm) from cultures in the presence of antigen divided by mean cpm of cultures with medium only (non-stimulated cells).

For the measurement of cytokine secretion in splenocyte cultures, the cells were plated at 2.5×10^6 cells/well (in duplicates) in 24-well plates (1 ml medium/well) and stimulated with OVA (100 μg/ml final concentrations in each well). Culture plates were incubated into a cell incubator (5% CO_2, 100% RH, 37 °C) for 48 h. Then, the supernatants were analyzed for the presence of IFNγ, IL-2, IL-4 and IL-10 by sandwich ELISA, using appropriate kits from Diaclone and following manufacturer's instructions.

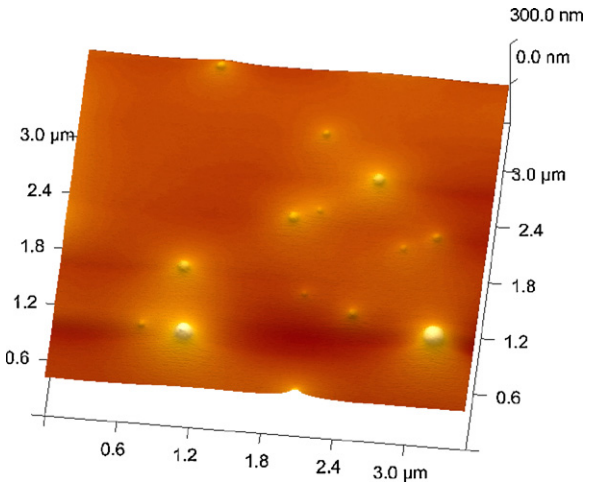

Fig. 1. AFM image of OVA-loaded nanoparticles.

2.8. Statistical analysis

The statistical significance of the differences between groups was investigated using Student's *t*-test for comparison of unpaired two samples and analysis of variance (ANOVA) for comparison of more than two samples (Statgraphics Plus 4 software). Differences were characterized as significant when $p < 0.05$.

3. Results

3.1. Characterization of the nanoparticles

Based on the AFM images (Fig. 1), discrete nanoparticles of spherical shape were obtained. The basic physicochemical properties and loading of different nanoparticle batches are shown in Table 1. When ethyl acetate was used as polymer solvent, the average size and % loading did not differ from those nanoparticles prepared using dichloromethane. However, the encapsulation efficiency of OVA fell to less than half of that in nanoparticles prepared using dichloromethane. This is because the nanoparticle recovery (% yield) in the case of those prepared using ethyl acetate was reduced to about half of that of nanoparticles prepared with dichloromethane (Table 1). In order to achieve a satisfactory recovery of nanoparticles and OVA encapsulation efficiency, the batches of nanoparticles administered *in vivo* were prepared using dichloromethane as the polymer solvent.

Table 1
Basic physicochemical characteristics and loading properties of PLA/OVA nanoparticles.

Batch no.	Polymer solvent	Size (nm)	P.I.	Z-potential (mV)	Nanoparticles yield (%)	Nanoparticles loading (%)	Encapsulation efficiency (for OVA, %)
1	Dichloromethane	149	0.138	−21.7	47.52	7.94	22.63
2	Dichloromethane	156	0.180	−22.1	47.00	7.74	21.82
3	Dichloromethane	148	0.142	−27.6	54.27	9.06	28.52
4	Ethyl acetate	150	0.185	−26.2	24.43	8.40	12.24
5	Ethyl acetate	143	0.151	−23.7	27.14	6.32	10.24

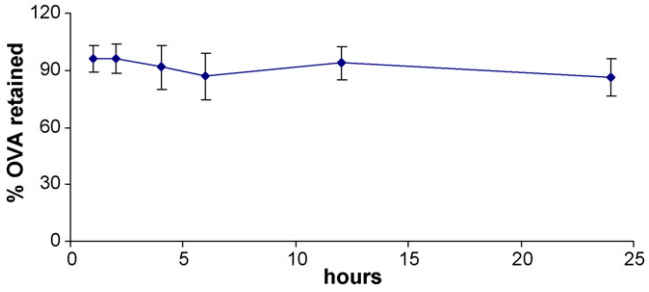

Fig. 2. OVA leakage from nanoparticles *in vitro* (PBS, 37 °C).

3.2. In vitro retention of OVA in nanoparticles

The retention of OVA in PLA nanoparticles over a period of 24 h is shown in Fig. 2. The nanoparticles retained more than 85% in average of their OVA content. A similar low rate leakage of OVA from PLGA nanoparticles has been reported by Coombes et al. (1996).

3.3. In vivo penetration of nanoparticles into the skin of mice

A dual fluorescence technique, which permits images to be recorded at two excitation/emission wavelength couplets, was applied in order to investigate the penetration of nanoparticles into the skin (Alvarez-Roman et al., 2004). In this technique, confocal images of the skin sample (visualized through its auto-fluorescence at 568 nm) were superimposed on images of the same skin sample (visualized at the excitation wavelength of the label of the fluorescent nanoparticles, i.e. at 488 nm). In the control skin samples, where nanoparticles had not been applied, only auto-fluorescence from the hair shafts could be observed with the red fluorescence detector at 568 nm (Fig. 3A). At 488 nm, very low auto-fluorescence could be seen with the green fluorescence detector (Fig. 3B). When the images were superimposed, only the auto-fluorescence of the hair shafts was observed (Fig. 3C). In the skin samples in which fluorescent nanoparticles had been applied, intense fluorescence from the FITC label (green color) can be seen with the green fluorescence detector (excitation 488 nm, Fig. 3E). When the images obtained with the red and the green fluorescence detector were superimposed, the fluorescence originating from the FITC label could be observed (Fig. 3F). FITC label on the surface of the skin as well as along the hair shaft inside the skin (at a depth of approximately 63 nm into the hair follicle) can clearly be observed. Fig. 3F indicates that the nanoparticles could gain access into the skin through the hair follicles.

3.4. Immune responses

In preliminary experiments, the optimum doses of antigen (OVA) and adjuvant (CT) to be used in the immunization protocol were determined by the proliferation assay 3 weeks after transcutaneous application of different doses of encapsulated antigen (OVA-loaded PLA nanoparticles) and adjuvant (data not shown). The maximum proliferative response was obtained when the dose of OVA and adjuvant were 200 and 50 μg, respectively.

The anti-OVA IgG responses elicited by the different OVA formulations are presented in Fig. 4. Following prime–boost immunization there were not significant differences ($p > 0.05$, paired comparison of same formulation at different times) in the anti-OVA response in the OVA solution and in the encapsulated OVA formulations (with or without adjuvant) (Fig. 4A). In contrast, the response to OVA when given in solution in the presence of CT was significantly increased after the boost ($p < 0.001$) (Fig. 4A). However, 2 weeks after the subcutaneous immunization with a sub-immunogenic dose of OVA, anti-OVA titres were significantly ($p < 0.001$) increased compared to the titres 4 weeks after priming in all groups of mice (comparison of data in Fig. 4B with those in Fig. 4A).

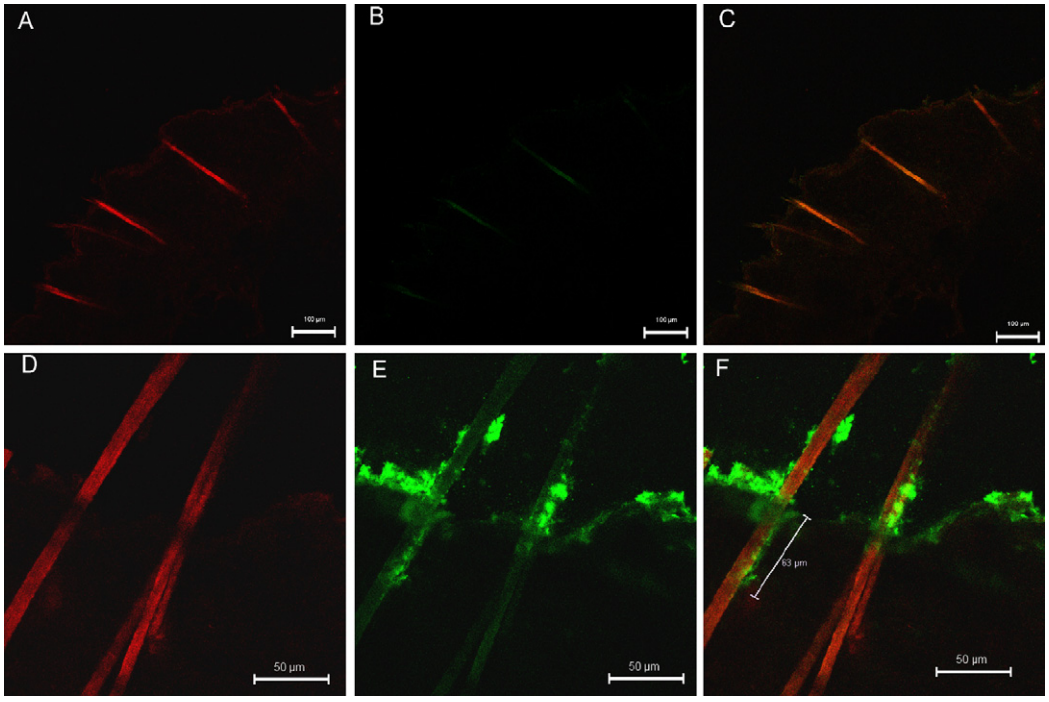

Fig. 3. Confocal laser scanning microscopy images of skin samples from mice in which fluorescent PLA nanoparticles had been applied epicutaneously: (A–C) are images of skin in which no nanoparticles had been applied (control images) and (D–F) are images of skin in which nanoparticles had been applied. The images (A and D) were obtained using laser excitation wavelength of 568 nm, the images (B and E) were obtained using laser excitation wavelength of 488 nm, the image (C) is obtained by superimposition of (A and B) images and the image (F) is obtained by superimposition of (D and E) images. The bar of 63 μm indicates the distance from the skin surface that the labeled nanoparticles have traveled.

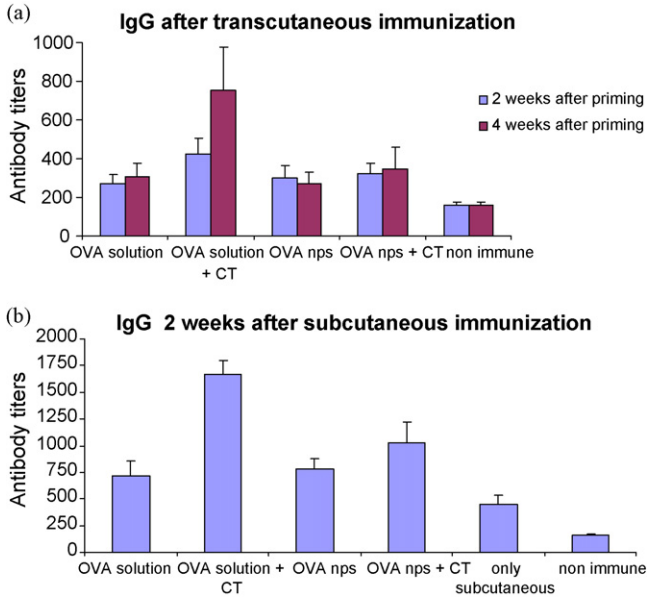

Fig. 4. IgG anti-OVA responses obtained with the different formulations: OVA solution = OVA solution in water, OVA solution + CT = OVA solution in water plus CT, OVA nps = OVA-loaded PLA nanoparticles, OVA nps + CT = OVA-loaded PLA nanoparticles plus CT, non-immune = non-immunized mice, only subcutaneous = mice immunized only subcutaneously. Bars indicate standard deviation ((A) $n = 7$, (B) $n = 4$).

The splenocyte proliferation ex vivo, for splenocytes isolated from mice immunized with different OVA formulations, is shown in Fig. 5. Stimulation indices higher than 2 were obtained, indicating the specificity of the immune response induced by the formulations tested.

The cytokine responses obtained with the different OVA formulations at 2 weeks after the booster transcutaneous immunization (i.e. at 4 weeks after transcutaneous priming) are shown in Fig. 6 (high cytokine responses were obtained with the positive control concanavalin A; they were not included in Fig. 6 for clarity). Following *in vitro* stimulation with OVA, the splenocytes of mice immunized with the OVA-loaded nanoparticles secreted a little higher IFN-γ (difference statistically insignificant, $p > 0.05$) and higher ($p < 0.001$) IL-2 levels than those immunized with the OVA aqueous solution. The OVA-loaded nanoparticles plus CT exhibited the highest IFN-γ and IL-2 responses, much higher than the other formulations tested. The only formulation which led to the secretion of significantly higher ($p < 0.001$) levels of IL-4 than the control (non-immunized mice) was the OVA-loaded nanoparticles plus CT (Fig. 6). All formulations led to the secretion of similar levels of IL-10 (Fig. 6).

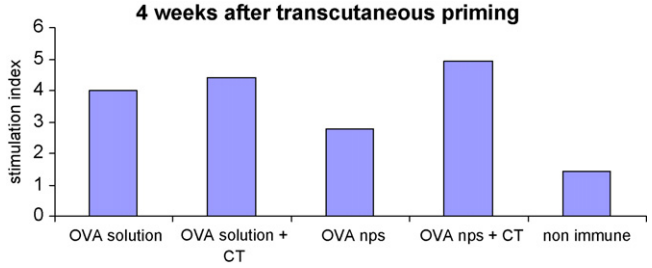

Fig. 5. Antigen-specific proliferative responses of splenocytes from mice immunized with the different OVA formulations (symbols as in Fig. 4).

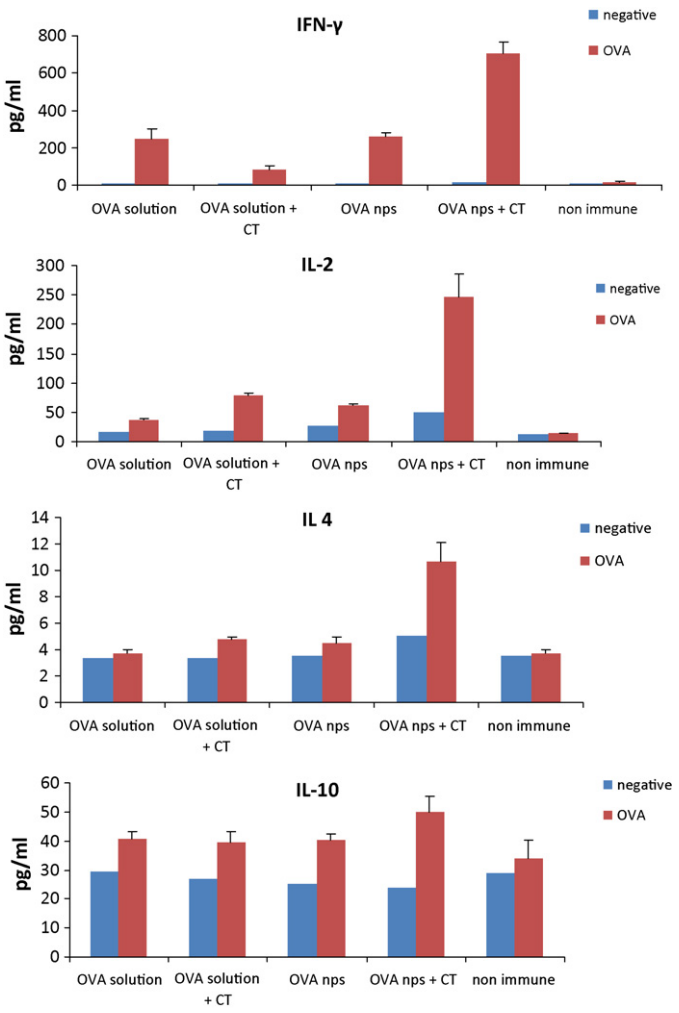

Fig. 6. Cytokine responses obtained with the different OVA formulations 4 weeks after primary transcutaneous immunization (symbols as in Fig. 4). Bars indicate standard deviation ($n = 3$).

4. Discussion

Recently, the topical delivery of antigens formulated into particulate delivery systems has evoked considerable interest. This is because these carriers can improve antigen permeation into the skin, protect antigen from degradation, promote sustained antigenic stimulation over prolonged period of time, and are not immunogenic. Certain particulate delivery systems, like PLGA microparticles of 1–10 μm diameter, can penetrate through the prehydrated stratum corneum and reach the basal layer of the epidermis (De Jalon et al., 2001). PLA and PLGA polymers are biocompatible and biodegradable, and have approval for clinical use in humans. Moreover, their composition can be adapted to encapsulate different types of antigens. Studies by Cui and Mumper (2001) have demonstrated that topical application of chitosan nanoparticles coated with plasmid DNA can elicit strong antibody and cellular responses to the expressed β-galactosidase antigen. Moreover, these responses could be further increased after topical co-application of plasmid DNA-coated nanoparticles together with CT as an adjuvant (Cui and Mumper, 2003). Alternatively, nanoparticles coated with plasmid DNA can be delivered directly into the epidermis using a jet injector and elicit potent immune responses to the encoded antigen (Cui et al., 2003; Mumper and Cui, 2003).

In the present study we examined the immune responses induced in mice following transcutaneous immunization with the

weak immunogen OVA, loaded into PLA nanoparticles. In subsequent experiments we investigated the ability of nanoparticles labeled with fluorescent FITC-albumin to penetrate into the mouse skin using confocal laser microscopy. The nanoparticles appeared capable of entering the skin through the duct of the hair follicles (Fig. 3). We did not observe other modes of nanoparticles entry into the skin in any of the skin samples examined. Our findings using an *in vivo* model are compatible to similar results obtained *in vitro* by others (Alvarez-Roman et al., 2004; Lademann et al., 2007).

Having established the capacity of nanoparticle formulation to breach the skin barrier, we then proceeded to evaluate the immune responses elicited after transcutaneous delivery of OVA-loaded PLA nanoparticles. The OVA-loaded nanoparticles induced similar total IgG responses as the OVA in solution (Fig. 4). With both modes of antigen delivery (aqueous solution and nanoparticles), the co-administration of CT adjuvant increased IgG response, especially that obtained with the OVA solution (Fig. 4). The augmentation of antibody responses against free OVA (OVA solution) by the co-administered CT (Fig. 4) is in accordance with previous findings with other protein antigens (Glenn et al., 1998; Scharton-Kersten et al., 2000). It is important to note that 2 weeks after the subcutaneous immunization with a sub-immunogenic dose of OVA, anti-OVA titres were significantly ($p < 0.001$) increased compared to the titres 4 weeks after priming in all groups of mice (comparison of data in Fig. 4B with those in Fig. 4A). This indicates the priming efficacy of transcutaneously applied encapsulated OVA to a challenging dose of OVA given via different route.

The encapsulated OVA (especially in the presence of CT) elicited relatively strong proliferative responses, indicating the effectiveness of nanoparticles to deliver antigen for antigen presentation (Fig. 5).

The OVA-loaded nanoparticles exhibited a little higher IFN-γ (however difference insignificant, $p > 0.05$) and higher IL-2 responses than the OVA solution whereas they elicited similar IL-4 and IL-10 responses with the OVA solution (Fig. 6). On the other hand the OVA-loaded nanoparticles plus CT induced much higher IFN-γ and IL-2 responses than all other formulations tested (Fig. 6). These results indicate that, as far as the cellular response is concerned, it may be advantageous to deliver the antigen in nanoparticle-encapsulated form rather than in free (aqueous solution) form. The increased IFN-γ and IL-2 levels obtained with the encapsulated forms of OVA (especially in the presence of CT) compared to the soluble forms of OVA may indicate a possible bias of immune response towards a Th1-type in the case of encapsulated OVA. The differences in the immunogenic behavior between the encapsulated OVA and free OVA may arise from the facilitated uptake and presentation of the encapsulated antigen by antigen-presenting cells (O'Hagan et al., 1997; Lofthouse, 2002). In order the antigen-loaded nanoparticles to manifest this different immunogenic behavior, the antigen should not leak from the nanoparticles before their phagocytosis *in vivo*. Indeed, according to the *in vitro* data (Fig. 2), OVA leaked only very slowly from the PLA nanoparticles.

Overall, the antibody and cytokine responses elicited by the OVA-loaded nanoparticles would justify further investigation of the potential of PLA nanoparticles as antigen delivery systems for transcutaneous immunization. The possibility of delivering vaccines in the future in a non-invasive fashion promises simplicity of delivery and higher rates of complacency that will enable successful outcomes from mass vaccination campaigns against infectious pathogens.

5. Conclusion

PLA nanoparticles with an average size around 150 nm appeared capable of entering into the mouse skin *in vivo* through the ducts of the hair follicles. OVA-loaded nanoparticles, when administered transcutaneously, elicited antibody responses comparable to those obtained with an equivalent dose of an aqueous OVA solution. Relatively high levels of IFN-γ and IL-2 were secreted from splenocytes of mice immunized with the OVA-loaded nanoparticles plus CT, following *in vitro* stimulation with antigen. This preferential stimulation of IFN-γ and IL-2 could be advantageous, particularly for the clearance of intracellular pathogens. Transcutaneous administration of OVA encapsulated in the PLA nanoparticles exhibited priming efficacy to a challenging dose of OVA given via different route. These findings indicate the potential of using PLA nanoparticles for transcutaneous antigen delivery.

Acknowledgement

The work was financed by "Karatheodori" program of University of Patras.

References

Alvarez-Roman, R., Naik, A., Kalia, Y.N., Guy, R.H., Fessi, H., 2004. Skin penetration and distribution of polymeric nanoparticles. J. Control. Release 99, 53–62.
Beignon, A.S., Briand, J.P., Muller, S., Partidos, C.D., 2001. Immunization onto bare skin with heat-labile enterotoxin of *Escherichia coli* enhances immune responses to coadministered protein and peptide antigens and protects mice against lethal toxin challenge. Immunology 102, 344–351.
Beletsi, A., Leontiadis, L., Klepetsanis, P., Ithakissios, D.S., Avgoustakis, K., 1999. Effect of preparative variables on the properties of PLGA-mPEG copolymers related to their application in controlled drug delivery. Int. J. Pharm. 182, 187–197.
Coombes, A.G.A., Lavelle, E.C., Jenkins, P.G., Davis, S.S., 1996. Single dose, polymeric, microparticle-based vaccines: the influence of formulation conditions on the magnitude and duration of the immune response to a protein antigen. Vaccine 14, 1429–1438.
Cui, Z., Baizer, L., Mumper, R.J., 2003. Intradermal immunization with novel plasmid DNA-coated nanoparticles via a needle-free injection device. J. Biotechnol. 102, 105–115.
Cui, Z., Mumper, R.J., 2001. Chitosan-based nanoparticles for topical genetic immunization. J. Control. Release 75, 409–419.
Cui, Z., Mumper, R.J., 2003. The effect of co-administration of adjuvants with a nanoparticle-based genetic vaccine delivery system on the resulting immune responses. Eur. J. Pharm. Biopharm. 55, 11–18.
De Jalon, E.G., Blanco-Prieto, M.J., Ygartua, P., Santoyo, S., 2001. Topical application of acyclovir-loaded microparticles: quantification of the drug in porcine skin layers. J. Control. Release 75, 191–197.
Glenn, G.M., Rao, M., Matyas, G.R., Alving, C.R., 1998. Skin immunization made possible by cholera toxin. Nature 391, 851.
Guidice, E.L., Campbell, J.D., 2006. Needle-free vaccine delivery. Adv. Drug. Deliv. Rev. 58, 68–89.
Igartua, M., Hernandez, R.M., Esquisabel, A., Gascon, A.R., Calvo, M.B., Pedraz, J.L., 1998. Enhanced immune response after subcutaneous and oral immunization with biodegradable PLGA microspheres. J. Control. Release 56, 63–73.
Kohli, A.K., Alpar, H.O., 2004. Potential use of nanoparticles for transcutaneous vaccine delivery: effect of particle size and charge. Int. J. Pharm. 275, 13–17.
Lademann, J., Richter, H., Teichmann, A., Otberg, N., Blume-Peytavi, U., Luengo, J., Weiß, B., Schaefer, U.F., Lehr, C.M., Wepf, R., Sterry, W., 2007. Nanoparticles—an efficient carrier for drug delivery into the hair follicles. Eur. J. Pharm. Biopharm. 66, 159–164.
Lofthouse, S., 2002. Immunological aspects of controlled antigen delivery. Adv. Drug. Deliv. Rev. 54, 863–870.
Men, Y., Gander, B., Merkle, H.P., Corradin, G., 1996. Induction of sustained and elevated immune responses to weakly immunogenic synthetic malarial peptides by encapsulation in biodegradable polymer microspheres. Vaccine 14, 1442–1450.
Mumper, R.J., Cui, Z., 2003. Genetic immunization by jet injection of targeted pDNA-coated nanoparticles. Methods 31, 255–262.
Nikou, K.N., Stivaktakis, N., Avgoustakis, K., Sotiropoulou, P.A., Perez, S.A., Baxevanis, C.N., Papamichail, M., Leondiadis, L., 2005. A HER-2/neu peptide admixed with PLA microspheres induces a Th1-biased immune response in mice. Biochim. Biophys. Acta: Gen. Subjects 1725, 182–189.
O'Hagan, D.T., Jeffry, H., Davis, S.S., 1993. Long-term antibody responses in mice following subcutaneous immunization with ovalbumin entrapped in biodegradable microparticles. Vaccine 11, 965–969.
O'Hagan, D.T., Ott, G.S., Van Nest, G., 1997. Recent advances in vaccine adjuvants: The development of MF59 emulsion and polymeric microparticles. Mol. Med. Today 3, 69–75.
Rosas, J.E., Pedraz, J.L., Hernandez, R.M., Gascon, A.R., Igartua, M., Guzman, F., Rodriguez, R., Cortes, J., Patarroyo, M.E., 2002. Remarkably high antibody levels and protection against P. Falciparum malaria in Aotus monkeys after a single immunization of SPf66 encapsulated in PLGA microspheres. Vaccine 20, 1707–1710.

Scharton-Kersten, T., Yu, J., Vassell, R., O'Hagan, D., Alving, C.R., Glenn, G.M., 2000. Transcutaneous immunization with bacterial ADP-ribosylating exotoxins, subunits, and unrelated adjuvants. Infect. Immun. 68, 5306–5313.
Smith, P.K., Krohn, R.I., Hermanson, G.T., Mallia, A.K., Gartner, F.H., Provenzano, M.D., Fujimoto, E.K., Goeke, N.M., Olson, B.J., Klenk, D.C., 1985. Measurement of protein using bicinchoninic acid. Anal. Biochem. 150, 76–85.
Streilein, W.J., 1983. Skin-associated lymphoid tissues (SALT): origins and functions. J. Invest. Dermatol. 80, 12s–16s.
Vogt, A., Combadiere, B., Hadam, S., Stieler, K.M., Lademann, J., Schaefer, H., Autran, B., Sterry, W., Blume-Peytavi, U., 2006. Epidermal CD1a+ cells after transcutaneous application on human skin. J. Invest. Dermatol. 126, 1316–1322.